HHS Public Access

Author manuscript

J Exp Zool B Mol Dev Evol. Author manuscript; available in PMC 2018 January 18.

Published in final edited form as:

J Exp Zool B Mol Dev Evol. 2016 December ; 326(8): 474–488. doi:10.1002/jez.b.22722.

Development shapes a consistent inbreeding effect in mouse crania of different line crosses

Mihaela Pavličev[1,*], **Philipp Mitteroecker**[2,*], **Paula M. Gonzalez**[3], **Campbell Rolian**[4], **Heather Jamniczky**[5,6], **Fernando Pardo-Manuel Villena**[7], **Ralph Marcucio**, **Richard Spritz**[8], and **Benedikt Hallgrimsson**[5,6,9]

[1]Cincinnati Children`s Hospital Medical Center and University of Cincinnati, Cincinnati, Ohio, USA

[2]Department of Theoretical Biology, University of Vienna, Althanstrasse 14, A-1090 Vienna, Austria

[3]Instituto de Genetica Veterinaria, University of La Plata, La Plata, Argentina

[4]Department of Comparative Biology, Faculty of Veterinary Medicine, University of Calgary, 3330 Hospital Dr. NW, Calgary, Alberta, Canada T2N 4N1

[5]Department of Cell Biology & Anatomy, University of Calgary, 3330 Hospital Dr. NW, Calgary, Alberta, Canada T2N 4N1

[6]McCaig Bone and Joint Institute, University of Calgary, 3330 Hospital Dr. NW, Calgary, Alberta, Canada T2N 4N1

[7]Department of Genetics, University of North Carolina, Durham, North Carolina, USA

[8]Department of Pediatrics and Human Medical Genetics and Genomics Program, University of Colorado School of Medicine, Denver, Colorado, USA

[9]Alberta Children's Hospital Research Institute, Department of Cell Biology & Anatomy, Faculty of Medicine, University of Calgary, 3330 Hospital Dr. NW, Calgary, Alberta, Canada T2N 4N1

Abstract

Development translates genetic variation into a multivariate pattern of phenotypic variation, distributing it among traits in a non-uniform manner. As developmental processes are largely shared within species, this suggests that the heritable phenotypic variation will be patterned similarly, in spite of the different segregating alleles. To investigate developmental effect on the variational pattern in the shape of the mouse skull across genetically differentiated lines, we employed the full set of reciprocal crosses (a.k.a. diallel) between eight inbred mouse strains of the Collaborative Cross Project. We used geometric morphometrics and multivariate analysis to capture cranial size and shape changes in 8 parentals and their 54 F1 crosses. The high heterozygosity generated in the F1 crosses allowed us to compare the multivariate deviations of

[+]Correspondence to: mihaela.pavlicev@cchmc.org, Cincinnati Children`s Hospital Medical Center and University of Cincinnati, Cincinnati, Ohio, USA. Tel: 513 308 2741.

[*]Joint first authors

DISCLOSURE DECLARATION

Authors Report no conflict of interest.

the F1 phenotypes from the expected mid-parental phenotypes in different haplotype combinations. In contrast to body weight, we found a high degree of non-additive deviation in craniofacial shape. Whereas the high phenotypic and genetic divergence of parental strains manifested in high dimensionality of additive effects, the non-additive deviations exhibited lesser dimensionality and in particular a strikingly coherent direction in shape space. We interpret this finding as evidence for a strong structuring effect of a relatively small set of developmental processes on the mapping of genetic to phenotypic variation.

Summary

Non-uniform distribution of heritable phenotypic variation can stem from past selection or developmental patterning. We demonstrate a highly consistent developmental effect in non-additive variation of mouse cranium regardless of genetic background.

Keywords

differential dominance; developmental constraint; pleiotropy; integration; multivariate quantitative genetics

Introduction

Heritable phenotypic variation underlies the evolvability of a population, and is determined by the presence of segregating alleles, and by the developmental processes that translate the genetic differences between individuals into phenotypic differences. In this sense, development is commonly conceptualized as a genotype-to-phenotype (GP) map. Identification of the structuring effect of development on phenotypic variation, however, requires the examination of phenotypes across multiple alleles and genetic backgrounds. A breeding design, called diallel, used here offers an effective empirical system for this question. A diallel consists of a number of inbred parental lines and, in its full form, two reciprocal crosses between each pair of the inbred lines, representing both heterozygotes. Data used in the present study stems from crossing eight inbred strains of mice as a part of the Collaborative Cross project (Churchill et al., 2004, Chesler et al., 2008, Aylor et al., 2011, Welsh et al., 2012).

In this paper, we address the effect of the developmental structure on heritable variation in the mouse cranium by comparing multivariate variation across a series of related inbred line crosses. The vertebrate cranium is a particularly compelling structure, as the closely coordinated development of its anatomical components funnels genetic variation to a narrow range of coordinated spatial variation, resulting in a subset out of all theoretically conceivable forms (Moss and Young, 1960, Cheverud, 1982, Klingenberg, 2013). Consequently, the polymorphisms at single loci are associated with coordinated changes in *combinations* of multiple cranial parts, mediated by the structuring effect of developmental processes and physical constraints (Leamy et al., 1999).

Our use of the diallel differs from its initial purposes in animal and plant breeding (Hayman, 1954, Jinks, 1954, Griffing, 1956). The classic diallel analyses aim either at estimating the

genetic structure of an interbreeding population, from which the inbred parental lines are assumed to be a random sample of genotypes; or they aim at understanding the combining ability of different lines. In the first case, it is assumed that inbred lines were inbred without selection. It is also frequently assumed that only two alleles with major frequency per locus exist. In both of these analyses, the additive effect of the haplotype is estimated as the average effect across different F1 (or P+F1) combinations. This expectation serves as the theoretical reference point from which to measure the non-additive deviations of the F1 phenotypes in the crosses. The classical analysis of diallel on the same population as used here has been reported previously (Percival et al. 2015). While these approaches have been useful for choosing the best crosses to optimize a specifically targeted trait, they reveal less about the structuring of the multivariate variation and the general evolvability. In fact, a method that sets the average non-additive deviations *a priori* to zero prevents detection of consistent directional deviations. Moreover, the focus on additive and non-additive *variance* is misleading for our purposes, as these aspects strongly depend on the choice of traits (as well as on the allele frequencies), as will be explained below.

By contrast, in this study we are interested in the individual rather than the statistical effects of allele substitutions. Therefore, instead of the average across all combinations of alleles, we use the midparental phenotypic value of the particular cross as the additive prediction for the F1 progeny, separately for each cross. We estimate the non-additive deviation as deviation from the midparental genotypic value and study the phenotypic distribution of these deviations across the F1 groups (see below).

A substantial source of non-additive deviation in the crosses between inbred lines is commonly due to heterosis or hybrid vigor. During the inbreeding, recessive alleles become combined in the homozygous state, and therefore inbred lines are often inferior in size and fitness to the lines with greater heterozygosity (see Discussion for additional effects across loci). In crosses between sufficiently divergent inbred lines, the reversion to heterozygosity results in abundant non-additive contribution to variation. If the *structuring* effect of development is weak, these deviations from the expected midparental values, represented as multivariate vectors, are expected to differ across crosses, as these lines were inbred separately, for different selective purposes. For a diallel cross of heterogeneous parental lines, such as ours, the non-additive deviation vectors may differ widely in direction in phenotype space. By contrast, if a common structuring effect of development dominates over the genetic background, we expect a shared tendency in direction of the deviations across genetic combinations. The pattern of consistency and the underlying morphological properties may thereby reveal the developmental processes that channel the genetic variation in the diallel.

Additive and non-additive effects on multivariate phenotypes

The classic concepts in quantitative genetics are formulated in the context of single traits. Morphological variation in parts of an integrated structure, such as the cranium, is interdependent due to developmental, spatial, and functional relationships. Such complex structures therefore require a multivariate approach. Here we use geometric morphometric shape descriptors (landmark shape coordinates), which are particularly unsuited for separate

biological interpretation – rather the analyses encompass the space of all possible linear combinations of variables (Bookstein, 1991, Adams et al., 2004, Hallgrimsson et al., 2009a, Mitteroecker, 2009). In Figures 1 and 2, we briefly outline the extension of the univariate genetic concepts to multiple traits (in simple Euclidian geometry, but some of the concepts extend to more general affine vector spaces as well; Huttegger and Mitteroecker, 2011).

For continuous univariate phenotypic variables, the additive genetic effect (*a*) of an allele substitution is conceptualized as half the difference between the average phenotypic values of the alternative homozygous genotypes (i.e., homozygote genotypic values; Figure 1A). When considering multiple traits, genotypic values can be represented by points in a multivariate phenotypic space, and vectors describing the effects of allele substitutions can differ both in length and direction. If the original measurements are considered distinct traits, directions in phenotype space that are oblique to a trait axis represent pleiotropic genetic effects (Figure 1B). For measurements that are not interpretable separately, as in geometric morphometrics and most image analysis approaches, the concept of pleiotropy is more ambiguous. The common notion of pleiotropy as an evolutionary constraint arises from the assumption that the direction of the genetic effect vector in phenotype space (the relative effects on multiple traits) is less evolvable than the length of this vector, depicting the overall effect size (Pavlicev et al., 2008, Pavlicev and Cheverud, 2015). Further, the dominance (*d*) of an allele is measured as deviation of the heterozygote genotypic value from the midpoint between the homozygous phenotypes (Figure 1C). For a single trait, the dominance is a scalar (hence the terms “underdominance” and “overdominance”), whereas it is a multivariate vector with length and direction for mulivariate traits. Dominance can thus affect only the magnitude, only the direction (Figure 1E), or both (Figure 1D). Dominance with respect to direction means that the effects of the single allele substitutions at a locus differ in their pleiotropic pattern, i.e., in their relative effects on the traits (differential dominance: (Klingenberg et al., 2001, Ehrich et al., 2003, Kenney-Hunt and Cheverud, 2009); differential epistasis: (Cheverud et al., 2004).

Importantly, this multivariate view reveals the significance of the choice of traits for the analysis and evolutionary interpretation of genetic variation, in particular with respect to assessing additive and non-additive effects (Figure 2). The presence of bivariate dominance in Figure 2 can be interpreted as anything from co-dominance to over-dominance or under-dominance when projected on different univariate subspaces (Klingenberg, Leamy, Routman and Cheverud, 2001). The choice of the trait (sub)space thus crucially determines the type of reported effects. This problem is particularly pertinent when the studied variables are not discernable biological traits (such as the length of the long bone), but arbitrary directions in a high-dimensional phenotype space.

In addition to the above considerations of genetic effects on multivariate phenotypes, a diallel cross differs in that not single loci, but the whole haplotypes segregate in F1. The genetic effects therefore cannot be attributed to single loci but are aggregates across many loci and include interactions between different loci (epistasis). For this reason, we refer to the “deviation from additivity” rather than specifying the source as dominance or epistasis. Furthermore, the multiple haplotypes (as opposed to only two alleles in above examples)

enable that the effect of haplotype substitutions can be measured in different combinations (i.e., allele/haplotype B combined with C, D, E).

MATERIAL AND METHODS

Strains

This study was performed on a diallel cross consisting of eight commercially available inbred mouse strains and an almost complete set (except for two) of their F1 crosses. The parental haplotypes will be denoted here by the letters A-H for simplicity, the corresponding full strain names are listed in Table 1. The strains AA-EE were generated by crossing other lines, mostly of lab mouse (*Mus musculus domesticus*), followed by selection and subsequent inbreeding. FF-HH are wild-derived strains that were generated from small numbers of wild animals of the subspecies *M. m. castaneus, M. m. musculus*, and *M. m. domesticus*, respectively, and subsequently inbred. These eight parental strains are the founders of the Collaborative Cross (Churchill et al. 2004, Chesler et al. 2008, Aylor et al. 2011, Welsh et al. 2012). Mice from the F1 generation were housed 2–5 animals per cage and had unlimited access to standard laboratory chow (LabDiet 5K52) and acidified drinking water. Individuals were sacrificed at approximately same age, averaging 72 days.

In our data only two of the F1 crosses are missing, resulting in the nearly full diallel of 62 strains. Each of the strains is represented by an average of 20 (range 16–29) genetically identical individuals (apart from potential spontaneous mutations). In total, 1211 individuals were included in the study after obvious outliers have been removed (of 1255 animals total). The distribution of individuals among strains and sexes are provided in Supplementary Table 1.

Phenotypes

All crania were micro CT-scanned (Scanco Viva-CT40, Scanco Medical AG, Basserdorf, Switzerland) at 35μm resolution (70 kv, 160 mA, 500 projections). Fifty-four three-dimensional landmarks, shown in Figure 3, were digitized using Analyze 3D (http://www.mayo.edu/bir/). Measurement error variances calculated by repeated measurement of the same individuals were less than 1.2% (Hallgrimsson et al., 2004b, Hallgrimsson et al., 2006). All three-dimensional landmark configurations were superimposed by a Generalized Procrustes Analysis, standardizing for position, scale and orientation of the configurations (Rohlf and Bookstein, 1990, Mitteroecker et al., 2013). Each configuration was averaged with its relabeled reflection, and the resulting symmetrized shape coordinates were used for further statistical analysis (Mardia and Bookstein, 2000, Mitteroecker and Gunz, 2009). Overall cranial size of each individual was computed as centroid size (CS), the square root of the summed squared distances between every landmark and their centroid (average landmark position). Asymmetry (within-individual variation) and canalization (between-individual variation) are addressed elsewhere (Gonzalez et al., 2016).

Statistical results based on the shape coordinates were represented by three-dimensional surface reconstructions. Using the thin-plate spline algorithm (Bookstein, 1989), the vertices of the triangulated surface of one mouse cranium was warped towards the corresponding

target configuration based on the measured landmarks. All morphometric and statistic analyses were performed in Mathematica 9.0 (Wolfram Research, Inc.) using routines programmed by Philipp Mitteroecker and Philipp Gunz.

Quantitative genetic analysis of shape and size

Throughout the study, we use midparental values as F1-specific expectations from which to estimate F1-specific deviation. The model underlying this approach is

$$x_{ij}=u_{ij}+s_{ij}+r_{ij}+e_{ij}, \quad (1)$$

where x_{ij} is the mean genotypic value of individuals with parental alleles i and j, s_{ij} is the average deviation from the midparental value of strains ii and jj, such that $s_{ij}=s_{ji}$, and r_{ij} is the reciprocal effect with respect to reciprocal combinations of alleles i and j, so that $r_{ij}=-r_{ji}$. The error term is denoted by e_{ij}. When possible, the deviation is shown for the separate F1 crosses, instead of the mean deviation of the two reciprocal crosses. Note that in this model the F1-specific reference, u_{ij}, is taken as the midparental value $u_{ij}=(x_{ii}+x_{jj})/2$.

Genetic effects on size: cranial size and body weight—We measured animal size using body weight and centroid size of the cranial landmarks, and analyzed the univariate genetic effects on these measures. The females of strain EE (*New Zealand Obese*) were older than those of other strains when the phenotypes were measured. Even though animals of all strains have reached their adult size, this strain is particularly prone to further weight gain beyond skeletal maturity, and hence age may confound the results. We therefore excluded this line from the analysis of genetic effects on body weight. Animals of all other strains were of similar age. The raw data (images as well as measured coordinates) is available at Facebase (https://www.facebase.org/).

Genetic effects on shape—We explored genetic effects on shape by a principal component analysis (PCA) of the 8 parental and 54 offspring group mean shapes. Separately, the distribution of multivariate dominance effects (i.e. deviation from additivity) was analyzed by a PCA of the vectors of multivariate shape deviations of the offspring group means from their corresponding parental midpoint. In contrast to the group means, these deviation vectors share a meaningful origin (representing no deviation from additivity) and hence the PCA of these vectors was computed by a singular value decomposition (SVD) of the uncentered matrix of deviation vectors. The resulting components maximize variation around the origin, not around the sample mean as in ordinary PCA, and thus also represent the average effect. The average of these vectors, i.e., the common pattern of dominance, was visualized by deformations of the three-dimensional surface of one mouse skull. We repeated these analyses after removing allometry (see Figures S1 and S2 in Supplementary material) by projecting the data onto the subspace perpendicular to the allometry vector, which was estimated by pooled within-group regression of the shape coordinates on centroid size (Burnaby, 1996, Mitteroecker et al., 2004).

Scalar estimates of multivariate heritability and genetic variance components would pool over all variables and conceal differences in genetic variance between different shape

features. To determine the phenotypic dimension with the highest proportion of genetic variance relative to environmental variance (as a proxy for broad-sense heritability), we computed an eigenanalysis of the covariance matrix of group means **B** *relative* to the pooled within-group covariance matrix **W** (Bookstein and Mitteroecker, 2014). The first relative eigenvector, which is the first eigenvector of the matrix product $\mathbf{W}^{-1}\mathbf{B}$, is the shape feature (linear combination of shape variables) with the highest ratio of genetic to environmental variances. This maximal ratio equals the first eigenvalue of $\mathbf{W}^{-1}\mathbf{B}$. Similarly, we identified the direction with minimum ratio of genetic to environmental variances (the last relative eigenvector) and other directions with an intermediate ratio (Roff, 2000, Klingenberg et al., 2010, Bookstein and Mitteroecker, 2014).

RESULTS

Genetic effects on size

Mean body weights for all strains, separated by sex, are presented in the heat plots in Figure 4A. The most apparent genetic effects on body weight are the positive additive effect of the E haplotype, the moderate negative additive effect of haplotypes F-H, and the moderate negative effect of inbreeding. The effect of the E haplotype on body size appears stronger when the haplotype comes from the mother. Genetic effects on body size appear of similar magnitude and pattern in males and females. Figure 4B shows mean cranial centroid size across the strains and sexes. The positive effect of haplotype E on cranial size is similar to that on body weight. The effect of inbreeding is manifested in smaller crania of inbred lines, again to the exception of genotype EE. Also here, the effect of the E haplotype appears stronger when it comes from the mother.

Line EE is an exception in that the inbred line shows no negative inbreeding effect. In the case of body weight this result could be confounded by the higher age of female individuals (Methods), potentially cancelling the negative effect of inbreeding, however this explanation is not sufficient for the cranial centroid size.

We are particularly interested in F1-specific deviations from the midparental values. Figure 5A shows body weight deviations for all F1 as a fraction of the midparental phenotype, to make the effects comparable across strains. Noteworthy positive deviations are associated with haplotypes A-D, and in many of these crosses we observe overdominance (|d|>|a|, see Supplementary Table S2).

The pattern of mean-normalized dominance deviations for the centroid size is captured in the heat map in Figure 5B, for every cross. When averaged over all groups, the F1 groups are on average 5.0% larger than their additive predictions, which equals 1.2 standard deviations of centroid size when pooled over the full sample. This is much stronger dominance than for body weight (2% lager on average). Also overdominance is much more common for the centroid size than for the body weight and is present in most crosses, with some exemption of crosses with the line E (i.e., NZO line). The overall pattern, but not the extent, of deviations from midparental values in CS resembles that of body size. Deviations and additive effects for body size and centroid size are listed in Supplementary Table S2 for all crosses.

Genetic effects on shape

The first eight principal components (PCs) of shape have relatively similar variances and together account for 88.1 % of total variance among the 62 group mean shapes. For most components, the offspring group means are located in between the parental groups, indicating some degree of additive inheritance (Figure 6). However, there are marked deviations of the offspring mean shapes from the corresponding midpoints of their parental mean shapes. These deviations, represented by the gray lines, are the non-additive genetic effects; and can be due to dominance and epistasis, that is, due to the changed effect of an allele in different backgrounds at the same or at other loci. Since both change between parental and F1 generation, we will not differentiate between dominance and epistasis here but treat them together as non-additive effects. Furthermore, Figure 6 demonstrates effects due to the sex of the parent of origin, reflected by the divergence of the two vectors connecting each parental midpoint with the corresponding reciprocal genotypes (e.g., AB versus BA).

Figure 7 shows a principal component ordination of all the non-additive deviation vectors, clearly demonstrating the common tendency among these vectors. When the deviation vectors are scaled to unit length, their average has a length of 0.70, indicating a highly significant deviation from a uniform spherical distribution (Mardia and Jupp, 1999). For the unscaled non-additive deviation vectors, a test of sphericity clearly indicated an anisotropic distribution ($p<0.001$; Mardia et al., 1979). The average deviation vector (as an estimate of the shared pattern of non-additivity) is visualized as a shape deformation in Figure 8. The variation that falls along this deformation includes the relative size of the neurocranium, the width and length of the midface, and the angle of the petrous temporal from the midline. We found no specific pattern in the allele of origin effects.

The eigenvalue distribution of the parental groups (or their pairwise mid-values as additive predictions of the F1 groups) is not directly comparable to that of the multivariate deviations because they differ greatly in their degrees of freedom (7 versus 53). However, the almost linearly decreasing eigenvalues of the additive predictions contrast starkly with the steeply, non-linearly decreasing eigenvalues (squared singular values) of the non-additive deviations. This shows that the variance due to non-additive effects is concentrated in fewer dimensions and hence more tightly integrated than the variance due to additive effects (Figure 9).

Heritability of shape

To assess the multivariate pattern of heritability, we performed a relative eigenanalysis of the between-group covariance matrix (as an estimate of genetic variance and covariance), relative to the within-group covariance matrix (as an estimate of environmental variance and covariance). The scree plot of the relative eigenvalues is shown in Figure 10. The first resulting relative eigenvector, i.e., the shape pattern with maximal ratio of genetic to environmental variance, is visualized in Figure 11. The shape variation that corresponds to the first relative eigenvector involves primarily variation in the relative sizes of the neurocranium and the face. In particular, the neurocranium varies in height and globularity along this axis. The width of the anterior midface, length of the molar row, and flaring of the zygomatic processes also vary along this axis. The second relative eigenvector corresponds

to width rather than height of the neurocranium, width of the midface, and length or the face. The last relative eigenvector reflects the shape feature with maximal environmental variance relative to genetic variance. Here, facial, basicranial and neurocranial width along with facial length vary most prominently.

Allometry

As we observed an inbreeding effect on cranial size (on average, parental lines were smaller than hybrid lines), we considered whether the observed shape differences between the parental inbred lines and the F1 lines are due to allometry, *i.e.*, an indirect effect of the size differences. We estimated average within-group allometry by a pooled within-group regression of shape on centroid size. Within each group, larger skulls, on average, have relatively smaller and less globular neurocrania, relatively longer, narrower faces, and more flexed basicrania (Figure 12 upper row). When removing the effect of allometry from the data, the non-allometric dominance vectors still show a common tendency, even though less pronounced as compared to the original data (not shown). The average deviation from additivity after removal of allometry is visualized in Figure 12 (lower row). Here, the largest changes involve relative facial length and width, relative length of the cranial base, and the angle of the face to the neurocranium. Removing allometry had essentially no effect on the relative eigenanalysis.

Overall additive vs. non-additive variance

To compare the relative magnitudes of additive and non-additive effects, we computed the average of the squared half distances between all pairs of parental group means (which is proportional to the additive genetic variance in this “population”) and the average squared dominance deviation. The ratio of this non-additive to additive mean sum of squares was 0.92 for cranial shape, 1.53 for cranial size, and 0.16 for weight.

DISCUSSION

The main aim of this study was to assess the effect of developmental structure on the distribution of genetic variation. We used the cranial measurements from a large set of mice, bred in a diallel cross of eight inbred lines. We find additive and non-additive components of genetic effects on overall size as well as on three-dimensional shape of the mouse cranium. The magnitude of non-additive effects, relative to additive effects, is larger for cranial size and shape than for body weight. Additive genetic effects in these crosses manifest themselves in the distribution of lines in the phenotypic space, the parental lines but not F1 crosses mapping to the outermost space, representing the distinct phenotypes of these lines. To estimate the effect to which development affects the phenotype, we focused on the deviation of the realized cranial shape in the F1 crosses from the additive predictions based on midparental values. Overall, we found that this deviation manifests a consistent phenotypic direction across different allelic combinations, regardless of the direction of additive effects, thus encompassing a much lower-dimensional subspace of the phenotype space than the additive effects. Non-additive variation in skull shape thus exhibits considerably more similarity across the diallel – an unexpected degree of common structure – as compared to the additive shape variation.

We use the pattern of genetic effects as the proxy for the developmental structure that directs the distribution of genetic variation among traits. It should be emphasized that while genetic effects reported here reflect the structure of the genotype-phenotype map, the results are not to be directly interpreted as proportion of additive and non-additive variance components in a wild population. In addition to the values of genetic effects, population variance is determined by the allele frequencies. Allele frequencies in this diallel cross are artificial, maximizing detectability of non-additive effects in statistical terms. As frequencies change, the non-additive effects of the same magnitude result in different variance proportions, because they contribute not only to non-additive, but also to additive genetic variance (Cheverud and Routman, 1995).

Multivariate deviation is inflated in F1 crosses of inbred lines: heterosis and pleiotropy

Deviation from additivity in the F1 between inbred lines surfaces as heterosis – the outperformance of the heterozygote progeny over both parentals in some trait or fitness – and reflects the deleterious effect of inbreeding as well as the presence of dominance and epistasis (Kristensen et al., 2010). Dominance (at least in univariate systems) is considered to reflect the robustness of physiology and development in organisms carrying wild type alleles ("safety margin", Wright, 1929, Wright, 1934, Kacser and Burns, 1981, Bourguet, 1999), due to which deleterious alleles are neutral with respect to the outcome of the process. As a consequence, deleterious alleles are masked from selection and spread in the population when combined with wild type alleles in heterozygous individuals. When combined in a homozygote, such as during inbreeding, these alleles, however, do affect the phenotype. Fully inbred lines further potentiate the situation, because the effects of recessive homozygotes accumulate across multiple loci. In addition to within loci, the analogous buffering effects occur also *between* different loci, and are similarly broken down in inbreeding.

Another source of multivariate deviation in F1 is *pseudo-pleiotropy* due to linkage. As shown in Fig. 1d, a change in direction of genetic effect manifests when the dominance effects on the two traits affected by the pleiotropic locus differ. In F1, whole haplotypes segregate; the pleiotropic and differential dominance effects of the loci thus accumulate. In addition, because of the lack of effective recombination in F1, many non-pleiotropic loci with dominance co-segregate. For example a locus affecting only trait A, and a locus affecting only trait B, are now combined into a single pseudo-pleiotropic effect on both traits because the whole haplotype acts as a single genetic factor, in which all *pleiotropic and non-pleiotropic* loci contribute to effective pleiotropy. Whenever the dominance effects of the loci on the traits differ (which is likely), they generate multivariate deviation in direction. This pseudo-pleiotropic effect potentiates the presence of multivariate dominance deviation in F1 of inbred lines, and may be expected to dissipate to some extent with recombination in further generations.

Relative contribution of non-additive deviation differs across traits

We found that the relative contribution of non-additive genetic effects is larger for cranial shape and size than for overall body weight. Within the vertebrate skeleton, the cranium is the spatially and developmentally most integrated structure, as is reflected in highly

correlated phenotypic variation. The morphological effects of allele substitutions on any one part therefore depend strongly on the phenotype of the affected cranial shape feature as well as on the phenotype of other, integrated features. This may result in non-linear effects of allele substitutions, and can generate non-additive genetic variance within a population. By contrast, the loci affecting overall body weight, which are likely more numerous than (but include) those affecting the cranium size, contribute to less spatially and developmentally interdependent phenotypic parts, reflected in a larger fraction of additive variance for body weight.

Interestingly, the previous study of genetic effects on morphological measurements across the whole mouse skeleton finds more prevalent multivariate dominance than analogous studies of mandibular traits in the same population (Ehrich, Vaughn, Koreishi, Linsey, Pletscher and Cheverud, 2003, Kenney-Hunt and Cheverud, 2009), however, it is not clear whether this overall effect is due to the higher number of skeletal variables rather than lesser integration. A more detailed study is necessary to address the relationship between the phenotypic integration and multivariate dominance of genetic effects. A potentially interesting consequence of such a relation would be the effect of integration on the maintenance of genetic variation, which results from the non-additive effects.

Directionality of deviation suggests restricted paths of phenotypic change

Even though the presence of non-additive deviation, and in particular non-additive deviation in direction of genetic effects is expected in this population, its consistent directionality across different crosses is highly remarkable. Despite a wide range of selection pressures to which the lines were exposed during their production and consequently a considerable variation among crosses, the multivariate dominance deviations show a clear common tendency, a consistent average pattern (Figure 7).

Allometry

Because of the strong genetic effects on size, some of the shape differences between parental and F1 populations may be ascribed to allometry. The average pattern of allometry involves changes in the relative size of the neurocranium and the face, facial length and width, and basicranial angle. Similar shape changes have been observed in growth hormone deficient mice and in mice treated with growth hormone (Gasperowicz et al., 2013). Hence, in both the Collaborative Cross and the growth hormone experiments, the integrated suite of allometric shape likely results from variation in the same underlying growth processes.

The number of different relevant growth processes in the cranium is much smaller than the number of genetic loci affecting cranial morphology (Hallgrimsson and Lieberman, 2008, Hallgrimsson et al., 2009b, Martinez-Abadias et al., 2012, Sanchez-Villagra et al., 2016). If the wide range of genetic variation is “funneled” by a few developmental processes, this will lead to similarities in the observed non-additive effects despite the different allele combinations involved. We thus suggest that the consistency of multivariate shape deviations across all F1 groups is likely a consequence of the perturbation of a similar set of canalized pathways during the inbreeding in at least this collection of strains.

Developmental basis

Clues to the developmental processes underlying the shared pattern of inbreeding effects can be inferred from Figure 8. This pattern of shape variation is qualitatively similar to patterns of population variation reported for the mouse cranium: strong axes of covariation between neurocranial and facial shape (Hallgrimsson et al., 2007, Lieberman et al., 2008). Similarly, studies involving mice with major mutations affecting chondrocranial size and brain size revealed a clear correlation between facial width, neurocranial height, and globularity (Hallgrimsson, Lieberman, Liu, Ford-Hutchinson and Jirik, 2007). In these studies, the axis of integrated shape change is generated by a series of mutations that are known to affect the relative rates of brain and chondrocranial growth. The one aspect in which the shape transformation observed in this study differs from the shape transformation produced in the mutant series is the absence of changes in basicranial angle.

Overall, the shape patterns of average non-additive deviation and allometry observed in the mouse diallel are reminiscent of the shape variation reported during inbreeding even in species distantly related to mouse. For example, inbreeding of natural populations of the Australian rat *Rattus villosissimus* in captivity resulted in smaller, broader, and shorter skulls (Lacy and Horner, 1996). These are also the shape features common among dog crania (Drake and Klingenberg, 2010). Moreover, decreased cranial size has been observed in inbred *Peromyscus polionotus* (Lacy and Alaks, 2013). Similar shape change has been proposed, in the context of the domestication syndrome, to be underlain by the neural crest cell deficit during early embryonic development (Wilkins et al., 2014), indicating the commonality of developmental changes during inbreeding and domestication (Sanchez-Villagra, Geiger and Schneider, 2016).

Heritability

Heritability differs drastically between different shape features. The ratio of between group to within group variances (corresponding to the ratio of total genetic to environmental variances as a proxy of broad-sense heritability) ranges from 18.0 to 1.0 in our sample. The shape features with maximal heritability are of relatively large scale, involving the height and width of the neurocranium, its globularity, and the length and width of the face. The similarities between the average non-additive shape pattern and additive components of shape variation indicate that both kinds of variation are strongly integrated by the same developmental processes acting in the skull. The shape feature with least heritability and, hence, with the strongest environmental influence is relatively local, affecting mainly the nasal bones.

Measuring deviation from additivity

Finally, it is noteworthy that the way of measuring the phenotype sets limits to genetic effects that we can detect and interpret biologically. Multivariate analyses pose additional challenges in this respect. Many complex phenotypes are of inherently multivariate nature. The larger the number of measurements, the more thoroughly can genetic effects be studied and the more likely are also non-additive effects identified. When complex structures are represented by a single or a few variables only, different choices of measurements can lead to strikingly different interpretations (Fig. 2). A powerful exploration of additive and various

non-additive effects thus requires a large number of measurements. At the same time, however, the expected distance between two points as well as the expected angle between two vectors increase with the number of random variables. It follows, that in high-dimensional phenotype spaces, measured deviations from additivity will tend to be large. In order to avoid this effect, the pattern of non-additive effects in multiple groups can be studied in a low-dimensional ordination, or the magnitude of effects can be expressed as a ratio of distances, such as the ratio of non-additive to additive squared effects in our study. Estimates based on single multivariate distances or angles should not be compared between samples comprising different numbers of variables.

Conclusion

Studying cranial shape in a large diallel panel of the Collaborative Cross mice, we have shown a surprising level of consistency in the direction of the deviations from the expected midparental values. These findings suggest a patterning of genetic variation by developmental processes, which resulted in highly consistent effects of inbreeding. Our results are consistent with work on craniofacial shape in mouse mutants, which shows that different genetic perturbations tend to produce similar and highly integrated effects on craniofacial shape. This has significant implications for understanding the genetics of complex morphological traits. Most importantly, the large and highly structured non-additive variation affects the evolvability of complex morphological structures and the maintenance of genetic variation.

Supplementary Material

Refer to Web version on PubMed Central for supplementary material.

Acknowledgments

MP acknowledges a postdoctoral fellowship from the Konrad Lorenz Institute for Evolution and Cognition Research and the support of the March of Dimes Prematurity Research Center Ohio Collaborative (#22-FY14-470). PM was supported by the Focus of Excellence grant “Biometrics of EvoDevo” of the Faculty of Life Science, University of Vienna. This work was also supported by NIH-NIDCR grants U01DE020054 to RS and BH, R01DE01963 and R01DE021708 to BH and RM, and NSERC 238992-12 to BH and MP.

References Cited

Adams DC, Rohlf FJ, Slice DE. Geometric morphometrics: ten years of progress following the 'revolution'. Ital J Zool. 2004; 71:5–16.

Aylor DL, Valdar W, Foulds-Mathes W, Buus RJ, Verdugo RA, Baric RS, Ferris MT, Frelinger JA, Heise M, Frieman MB, Gralinski LE, Bell TA, Didion JD, Hua K, Nehrenberg DL, Powell CL, Steigerwalt J, Xie Y, Kelada SN, Collins FS, Yang IV, Schwartz DA, Branstetter LA, Chesler EJ, Miller DR, Spence J, Liu EY, McMillan L, Sarkar A, Wang J, Wang W, Zhang Q, Broman KW, Korstanje R, Durrant C, Mott R, Iraqi FA, Pomp D, Threadgill D, de Villena FP, Churchill GA. Genetic analysis of complex traits in the emerging Collaborative Cross. Genome Res. 2011; 21:1213–1222. [PubMed: 21406540]

Bookstein F. Principal warps: Thin plate splines and the decomposition of deformations. IEEE Trans Pattern Anal Machine Intelligence. 1989; 11:567–585.

Bookstein F, Mitteroecker P. Comparing Covariance Matrices by Relative Eigenanalysis, with Applications to Organismal Biology. Evolutionary Biology. 2014; 41:336–350.

Bookstein, FL. Morphometric Tools for Landmark Data. Cambridge: Cambridge University Press; 1991.

Bourguet D. The evolution of dominance. Heredity (Edinb). 1999; 83(Pt 1):1–4. [PubMed: 10447697]

Burnaby TP. Growth-invariant discriminant functions and generalized distances. Biometrics. 1996; 22:96–110.

Chesler EJ, Miller DR, Branstetter LR, Galloway LD, Jackson BL, Philip VM, Voy BH, Culiat CT, Threadgill DW, Williams RW, Churchill GA, Johnson DK, Manly KF. The Collaborative Cross at Oak Ridge National Laboratory: developing a powerful resource for systems genetics. Mammalian genome : official journal of the International Mammalian Genome Society. 2008; 19:382–389. [PubMed: 18716833]

Cheverud JM. Phenotypic, genetic, and environmental morphological integration in the cranium Evolution. international journal of organic evolution. 1982; 36:499–516.

Cheverud JM, Ehrich TH, Vaughn TT, Koreishi SF, Linsey RB, Pletscher LS. Pleiotropic effects on mandibular morphology II: differential epistasis and genetic variation in morphological integration. Journal of experimental zoology Part B, Molecular and developmental evolution. 2004; 302:424–435.

Cheverud JM, Routman EJ. Epistasis and its contribution to genetic variance components. Genetics. 1995; 139:1455–1461. [PubMed: 7768453]

Churchill GA, Airey DC, Allayee H, Angel JM, Attie AD, Beatty J, Beavis WD, Belknap JK, Bennett B, Berrettini W, Bleich A, Bogue M, Broman KW, Buck KJ, Buckler E, Burmeister M, Chesler EJ, Cheverud JM, Clapcote S, Cook MN, Cox RD, Crabbe JC, Crusio WE, Darvasi A, Deschepper CF, Doerge RW, Farber CR, Forejt J, Gaile D, Garlow SJ, Geiger H, Gershenfeld H, Gordon T, Gu J, Gu W, de Haan G, Hayes NL, Heller C, Himmelbauer H, Hitzemann R, Hunter K, Hsu HC, Iraqi FA, Ivandic B, Jacob HJ, Jansen RC, Jepsen KJ, Johnson DK, Johnson TE, Kempermann G, Kendziorski C, Kotb M, Kooy RF, Llamas B, Lammert F, Lassalle JM, Lowenstein PR, Lu L, Lusis A, Manly KF, Marcucio R, Matthews D, Medrano JF, Miller DR, Mittleman G, Mock BA, Mogil JS, Montagutelli X, Morahan G, Morris DG, Mott R, Nadeau JH, Nagase H, Nowakowski RS, O'Hara BF, Osadchuk AV, Page GP, Paigen B, Paigen K, Palmer AA, Pan HJ, Peltonen-Palotie L, Peirce J, Pomp D, Pravenec M, Prows DR, Qi Z, Reeves RH, Roder J, Rosen GD, Schadt EE, Schalkwyk LC, Seltzer Z, Shimomura K, Shou S, Sillanpaa MJ, Siracusa LD, Snoeck HW, Spearow JL, Svenson K, Tarantino LM, Threadgill D, Toth LA, Valdar W, de Villena FP, Warden C, Whatley S, Williams RW, Wiltshire T, Yi N, Zhang D, Zhang M, Zou F. Complex Trait C. The Collaborative Cross, a community resource for the genetic analysis of complex traits. Nature genetics. 2004; 36:1133–1137. [PubMed: 15514660]

Drake AG, Klingenberg CP. Large-scale diversification of skull shape in domestic dogs: disparity and modularity. Am Nat. 2010; 175:289–301. [PubMed: 20095825]

Ehrich TH, Vaughn TT, Koreishi SF, Linsey RB, Pletscher LS, Cheverud JM. Pleiotropic effects on mandibular morphology I. Developmental morphological integration and differential dominance. Journal of experimental zoology Part B, Molecular and developmental evolution. 2003; 296:58–79.

Gasperowicz M, Gonzalez PN, Hallgrimsson B, Cross JC. Placental adaptations in response to protein restricted diet. Placenta. 2013; 34:A28–A28.

Gonzalez PN, Pavlicev M, Mitteroecker P, Pardo-Manuel de Villena F, Spritz RA, Marcucio RS, Hallgrimsson B. Genetic structure of phenotypic robustness in the collaborative cross mouse diallel panel. Journal of evolutionary biology. 2016

Griffing B. Concept of general and specific combining ability in relation to diallel crossing systems. Aust J Biol Sci. 1956; 9:463–493.

Hallgrimsson, B., Boughner, JC., Turinsky, A., Parsons, TE., Logan, C., Sensen, CW., et al. Geometric morphometrics and the study of development. Sensen, CW., Hallgrimsson, B., editors. Sringer Verlag; 2009a.

Hallgrimsson B, Brown JJ, Ford-Hutchinson AF, Sheets HD, Zelditch ML, Jirik FR. The brachymorph mouse and the developmental-genetic basis for canalization and morphological integration. Evol Dev. 2006; 8:61–73. [PubMed: 16409383]

Hallgrimsson B, Dorval CJ, Zelditch ML, German RZ. Craniofacial variability and morphological integration in mice susceptible to cleft lip and palate. Journal of anatomy. 2004a; 205:501–517. [PubMed: 15610397]

Hallgrimsson B, Jamniczky H, Young NM, Rolian C, Parsons TE, Boughner JC, Marcucio RS. Deciphering the Palimpsest: Studying the Relationship Between Morphological Integration and Phenotypic Covariation. Evolutionary Biology. 2009b; 36:355–376. [PubMed: 23293400]

Hallgrimsson B, Lieberman DE. Mouse models and the evolutionary developmental biology of the skull. Integrative and comparative biology. 2008; 48:373–384. [PubMed: 21669799]

Hallgrimsson B, Lieberman DE, Liu W, Ford-Hutchinson AF, Jirik FR. Epigenetic interactions and the structure of phenotypic variation in the cranium. Evol Dev. 2007; 9:76–91. [PubMed: 17227368]

Hallgrimsson B, Willmore K, Dorval C, Cooper DM. Craniofacial variability and modularity in macaques and mice. Journal of experimental zoology Part B, Molecular and developmental evolution. 2004b; 302:207–225.

Hayman BI. The Theory and Analysis of Diallel Crosses. Genetics. 1954; 39:789–809. [PubMed: 17247520]

Huttegger S, Mitteroecker P. Invariance and meaningfulness in phenotype spaces. Evolutionary biology. 2011; 38:335–351.

Jinks JL. The Analysis of Continuous Variation in a Diallel Cross of Nicotiana Rustica Varieties. Genetics. 1954; 39:767–788. [PubMed: 17247519]

Kacser H, Burns JA. The molecular basis of dominance. Genetics. 1981; 97:639–666. [PubMed: 7297851]

Kenney-Hunt JP, Cheverud JM. Differential dominance of pleiotropic loci for mouse skeletal traits. Evolution; international journal of organic evolution. 2009; 63:1845–1851. [PubMed: 19566580]

Klingenberg CP. Cranial integration and modularity: insights into evolution and development from morphometric data. Hystrix. 2013; 24:43–58.

Klingenberg CP, Debat V, Roff DA. Quantitative genetics of shape in cricket wings: developmental integration in a functional structure. Evolution. 2010; 64:2935–2951. [PubMed: 20482613]

Klingenberg CP, Leamy LJ, Routman EJ, Cheverud JM. Genetic architecture of mandible shape in mice: effects of quantitative trait loci analyzed by geometric morphometrics. Genetics. 2001; 157:785–802. [PubMed: 11156997]

Kristensen TN, Pedersen KS, Vermeulen CJ, Loeschcke V. Research on inbreeding in the 'omic' era. Trends Ecol Evol. 2010; 25:44–52. [PubMed: 19733933]

Lacy RC, Alaks G. Effects of inbreeding on skeletal size and fluctuating asymmetry of Peromyscus polionotus mice. Zoo Biol. 2013; 32:125–133. [PubMed: 22814968]

Lacy RC, Horner BE. Effects of inbreeding on skeletal development of Rattus villosissimus. J Hered. 1996; 87:277–287. [PubMed: 8776876]

Leamy LJ, Routman EJ, Cheverud JM. Quantitative trait loci for early- and late-developing skull characters in mice: A test of the genetic independence model of morphological integration. American Naturalist. 1999; 153:201–214.

Lieberman DE, Hallgrimsson B, Liu W, Parsons TE, Jamniczky HA. Spatial packing, cranial base angulation, and craniofacial shape variation in the mammalian skull: testing a new model using mice. Journal of anatomy. 2008; 212:720–735. [PubMed: 18510502]

Mardia KV, Bookstein FL. Statistical assessment of bilateral symmetry of shapes. Biometrika. 2000; 87:285–3000.

Mardia, KV., Jupp, PE. Directional Statistics. Wiley; 1999.

Mardia, KV., Kent, JT., Bibby, JM. Multivariate analysis. London; New York: Academic Press; 1979.

Martinez-Abadias N, Mitteroecker P, Parsons TE, Esparza M, Sjovold T, Rolian C, Richtsmeier JT, Hallgrimsson B. The Developmental Basis of Quantitative Craniofacial Variation in Humans and Mice. Evolutionary Biology. 2012; 39:554–567. [PubMed: 23226904]

Mitteroecker P. The developmental basis of variational modularity: Insights from quantitative genetics, morphometrics, and developmental biology. Evolutionary biology. 2009; 36:235–247.

Mitteroecker P, Gunz P. Advances in Geometric Morphometrics. Evolutionary Biology. 2009; 36:235–247.

Mitteroecker P, Gunz P, Bernhard M, Schaefer K, Bookstein FL. Comparison of cranial ontogenetic trajectories among great apes and humans. J Hum Evol. 2004; 46:679–697. [PubMed: 15183670]

Mitteroecker P, Gunz P, Windhager S, Schaefer K. A brief review of shape, form, and allometry in geometric morphometrics, with applications to human facial morphology. Hystrix-Italian Journal of Mammalogy. 2013; 24:59–66.

Moss ML, Young RW. A functional approach to craniology. American journal of physical anthropology. 1960; 18:281–292. [PubMed: 13773136]

Pavlicev M, Cheverud JM. Constraints evolve: context dependency of genetic effects allows evolution of pleiotopy. Annual review of ecology, evolution and systematics. 2015; 46:413–434.

Pavlicev M, Kenney-Hunt JP, Norgard EA, Roseman CC, Wolf JB, Cheverud JM. Genetic variation in pleiotropy: differential epistasis as a source of variation in the allometric relationship between long bone lengths and body weight. Evolution; international journal of organic evolution. 2008; 62:199–213. [PubMed: 18005158]

Roff D. The evolution of the G matrix: selection or drift? Heredity. 2000; 84:135–142. [PubMed: 10762382]

Rohlf, FJ., Bookstein, FL. Proceedings of the Michigan Morphometrics Workshop. Ann Arbor: U. Michigan Museum of Zoology; 1990.

Sanchez-Villagra MR, Geiger M, Schneider RA. The taming of the neural crest: a developmental perspective on the origins of morphological covariation in domesticated mammals. R Soc Open Sci. 2016; 3:160107. [PubMed: 27429770]

Welsh CE, Miller DR, Manly KF, Wang J, McMillan L, Morahan G, Mott R, Iraqi FA, Threadgill DW, de Villena FP. Status and access to the Collaborative Cross population. Mamm Genome. 2012; 23:706–712. [PubMed: 22847377]

Wilkins AS, Wrangham RW, Fitch WT. The "domestication syndrome" in mammals: a unified explanation based on neural crest cell behavior and genetics. Genetics. 2014; 197:795–808. [PubMed: 25024034]

Wright S. The evolution of dominance. Am Nat. 1929; 63:556–561.

Wright S. Physiological and evolutionary theories of dominance. Am Nat. 1934; 68:24–53.

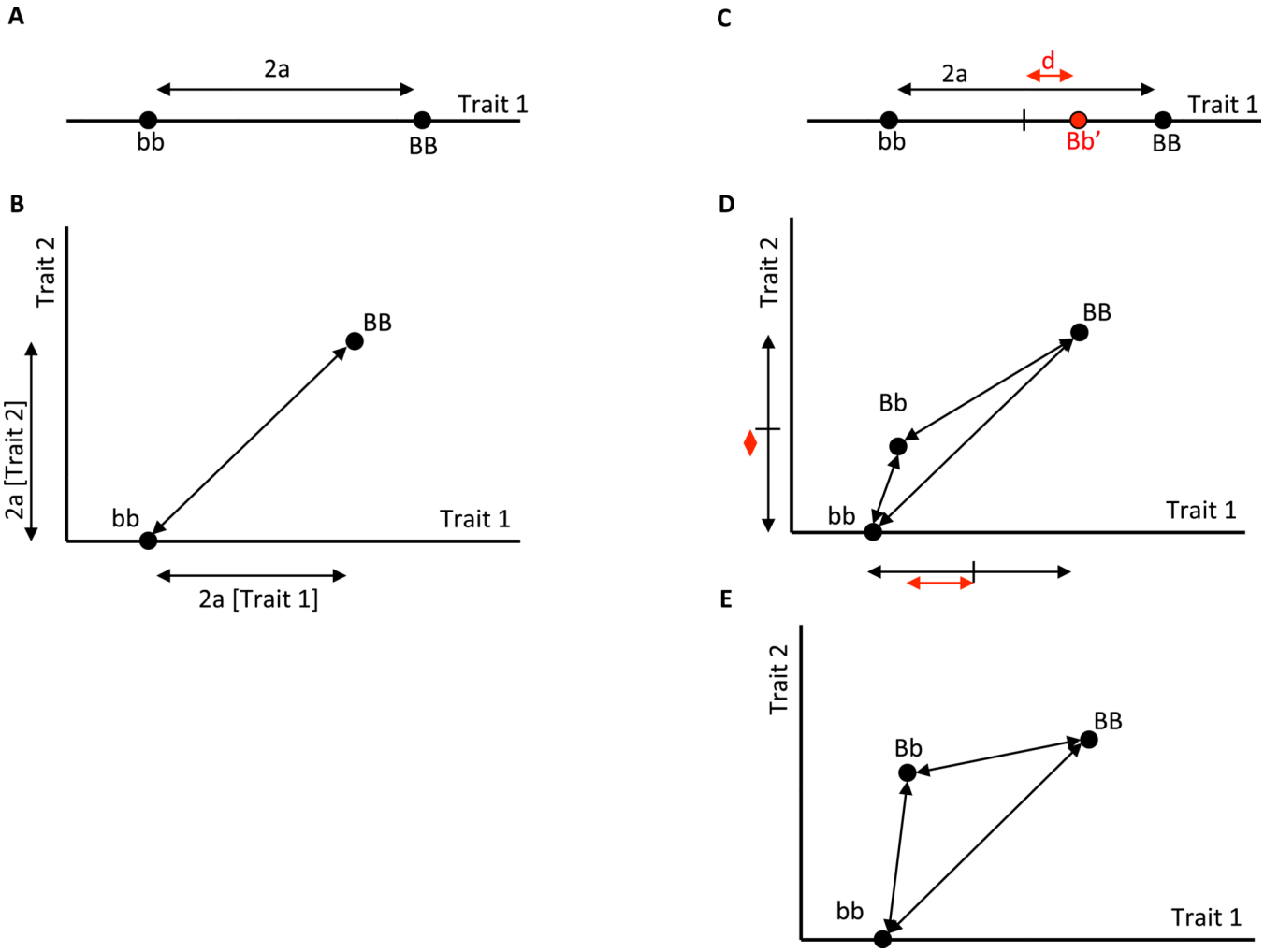

Figure 1.

(A) The additive effect *a* on a univariate trait (Trait 1) geometrically corresponds to half the length of the vector between the two phenotypic values that each represents the mean across individuals with homozygous genotypes. (B) In the multivariate case, phenotypes can be represented by points in a multivariate space. The additive pleiotropic effect on two traits is measured as half the distance between genotypes with respect to two traits. Vectors describing phenotypic differences between the genotypes can differ both in length and direction. The direction of a vector represents the relative effects on two or more phenotypic variables, and its length represents the overall magnitude of the effect. All directions oblique to any trait axis represent pleiotropic genetic effects (C) Deviation from additivity in heterozygote is called dominance (d, red), shown here in univariate case. Dominance is present when the effect of an allele substitution depends on the other allele at the same locus. Lack of dominance, or *codominance*, implies that the heterozygote phenotype (Bb) is at the midpoint between the homozygous phenotypes, and the dominance effect is measured as deviation of the heterozygote phenotype from this additive prediction. (D) For multiple measurements, dominance is a multivariate vector, of which both length and direction can depend on which alternative allele is present at the same locus. For example, the first

substitution B->b occurs in the presence of *B*, the second in the presence of *b*. The phenotypic effects of the two substitutions differ in magnitude as well as in direction. (E) a case of dominance, in which the heterozygote is at equal distance from the parentals yet dominance is present with respect to the direction of genetic effects.

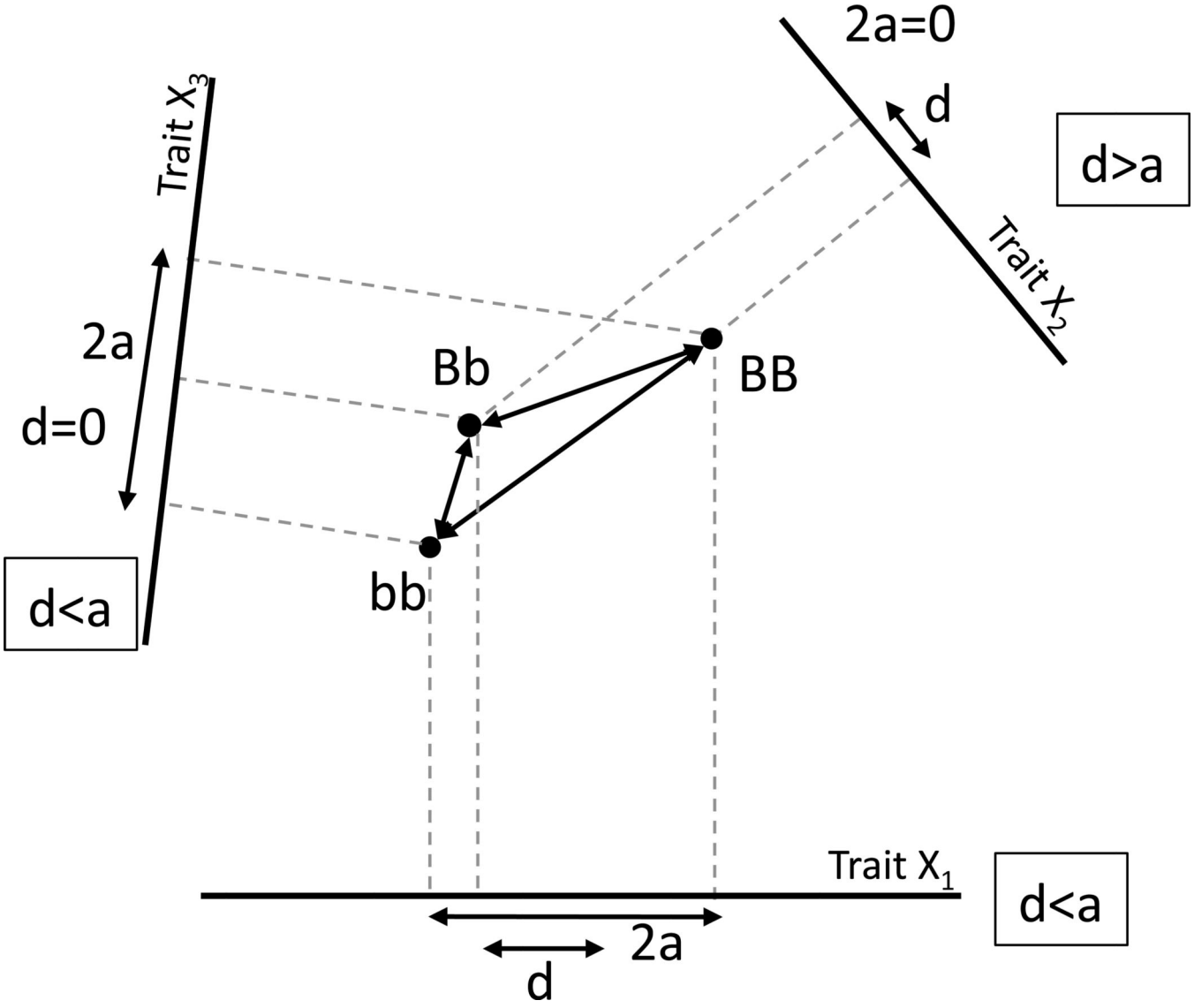

Figure 2.

Depending on the choice of phenotypic traits (represented by axes), various degrees of dominance and additivity can be inferred in the same system. For two measurements (horizontal and vertical axes, two-dimensional space), the three different choices shown here (the linear combinations X_1-X_3) differ substantially in their additive effect (*a*) and dominance deviation (*d*).

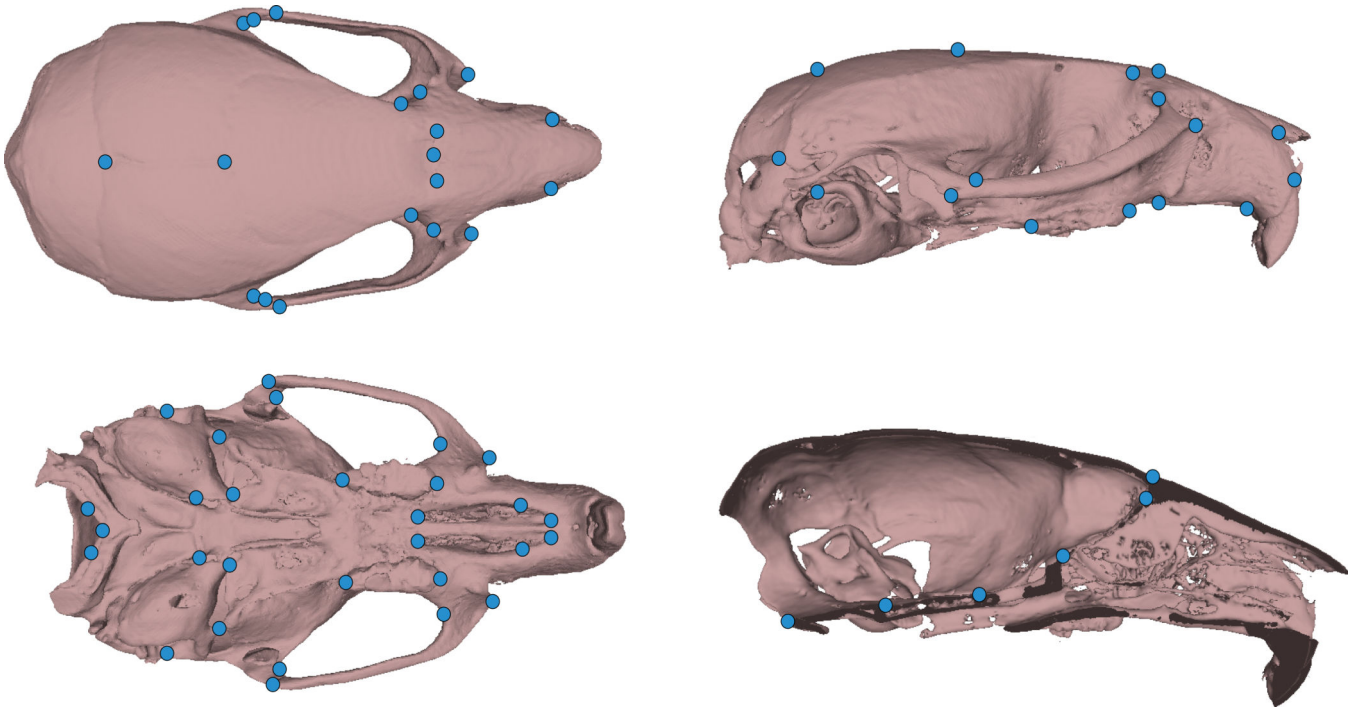

Figure 3.
3D Landmarks digitized for the mouse skulls in the sample. For details see Hallgrimsson et al. (2004a).

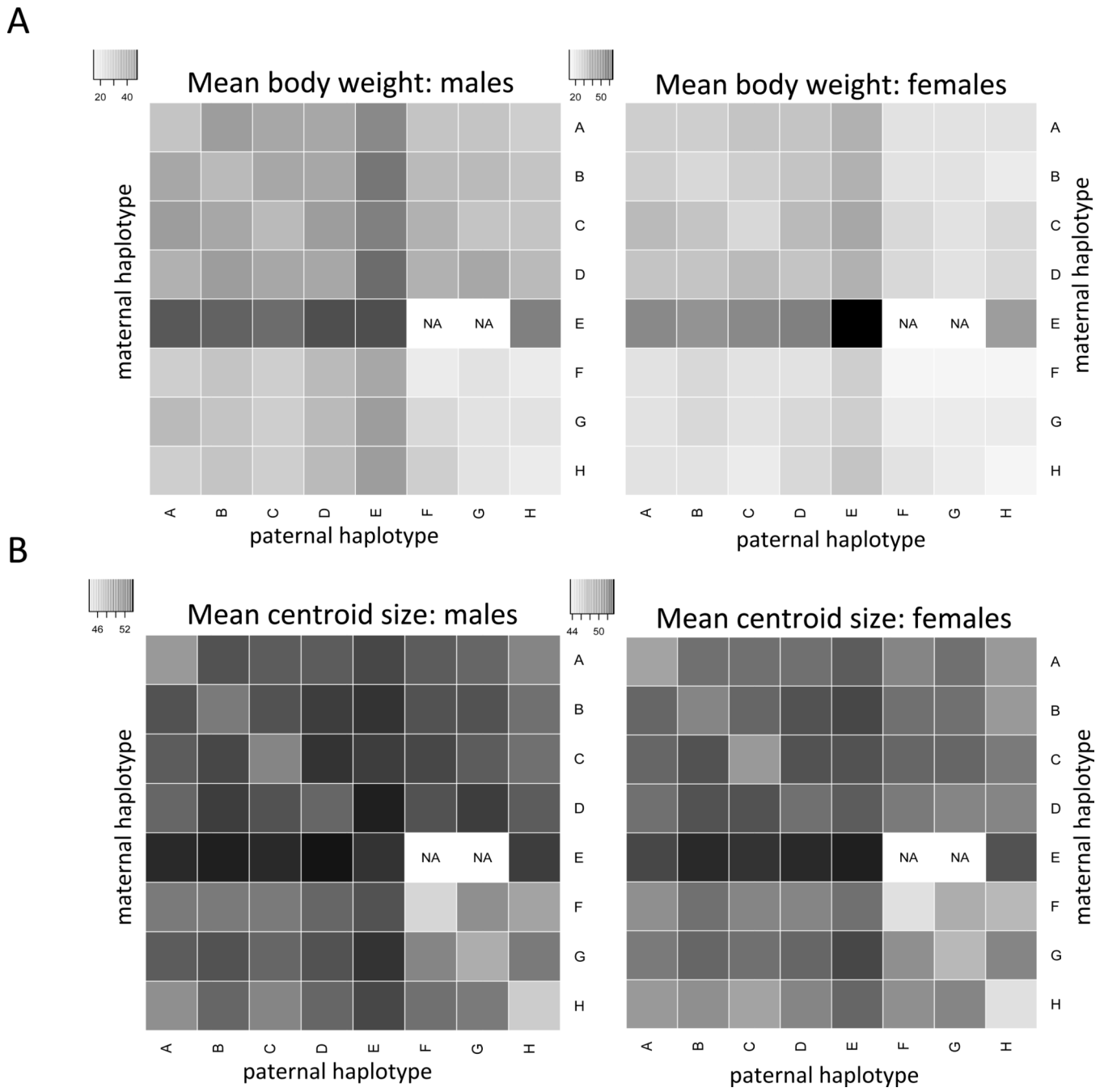

Figure 4.

Heat map of the mean body size for all genotypes, separately for males and females (A), and corresponding heat plot of the mean cranial centroid size for all genotypes (B). In these plots, each matrix element represents a strain, with inbred parental strains along the diagonal and F1 crosses in the off-diagonal elements. Asymmetry across the diagonal reflects differences between reciprocal combinations of parental haplotypes (i.e., parent of origin effect). The additive effects of alleles (Supplementary Table S2) are visible as consistent signature of distinct rows or columns, and the inbreeding effects are reflected in the

consistently lower or higher value of diagonal elements compared to the off-diagonal elements of the corresponding row or column. Sex effects are represented by the differences between the two sex-specific matrices.

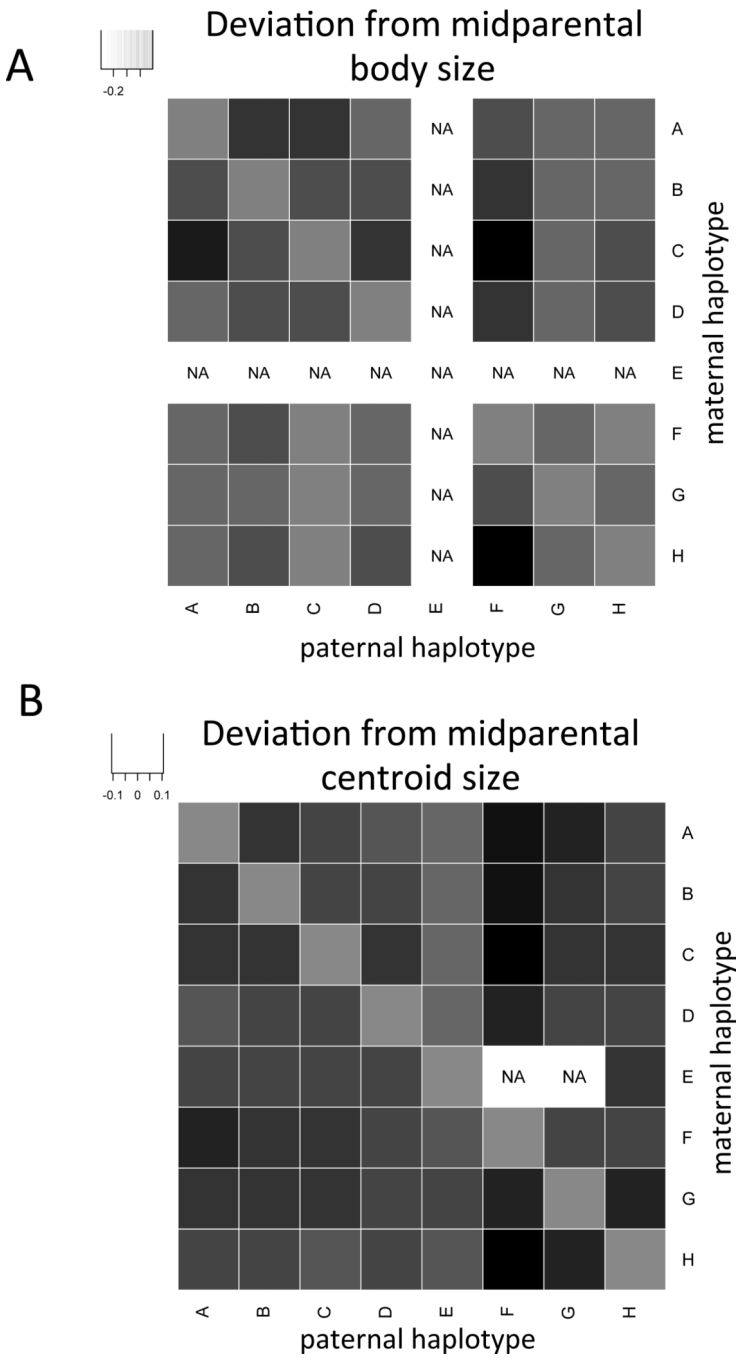

Figure 5.

Heat plots presenting (A) deviations from the midparental value for body size, and (B) deviation from the midparental value for centroid size. Values are expressed as a fraction of midparental value.

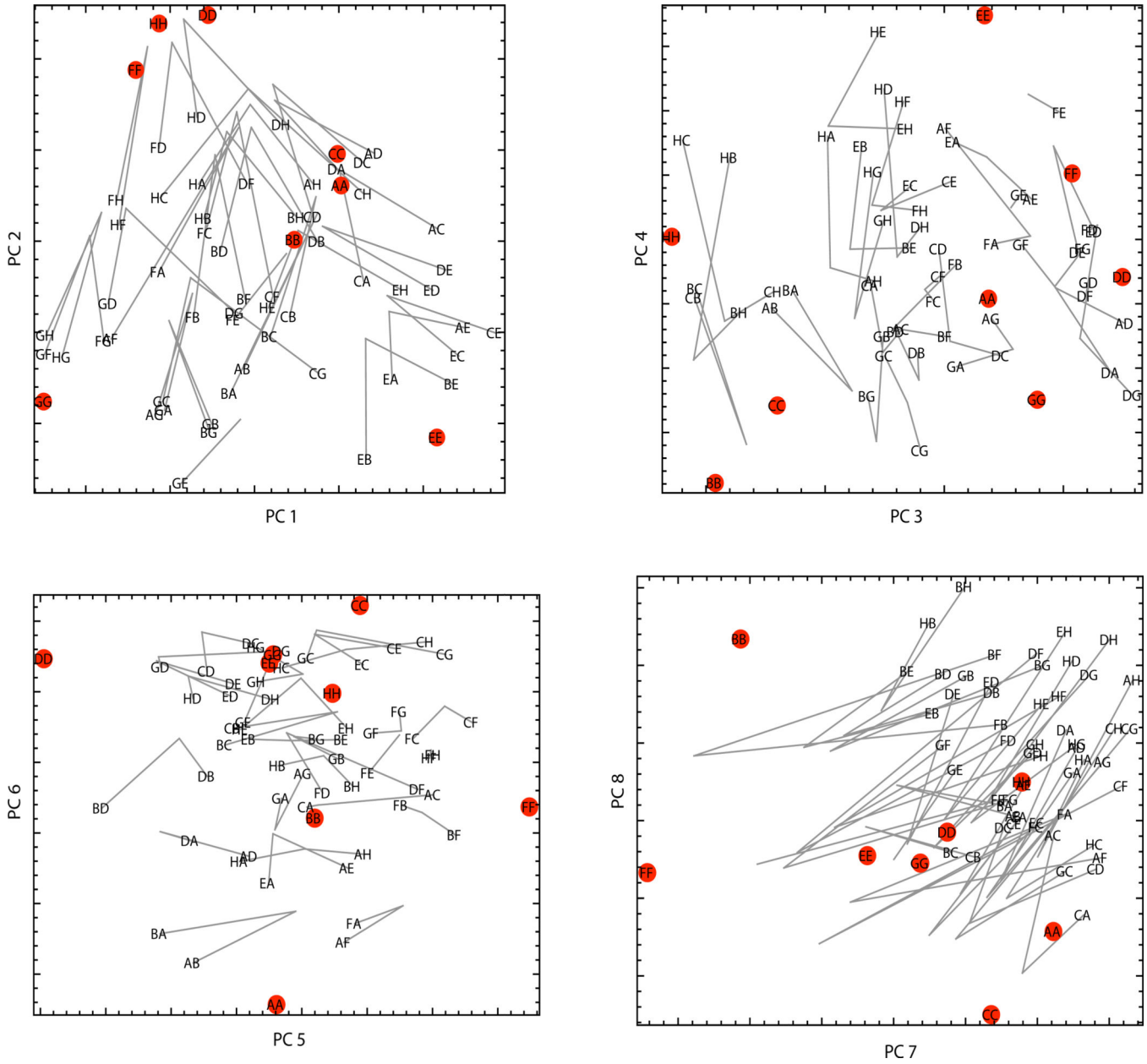

Figure 6.

Scatterplots of the first eight principal components (PCs) of the group mean shapes. The parental groups are marked by filled red circles. Every offspring group is connected to its corresponding parental midpoint by a gray line, which represents multivariate dominance. Note the common pattern of dominance (the share direction of the gray deviation vectors), especially along PCs 2 and 8.

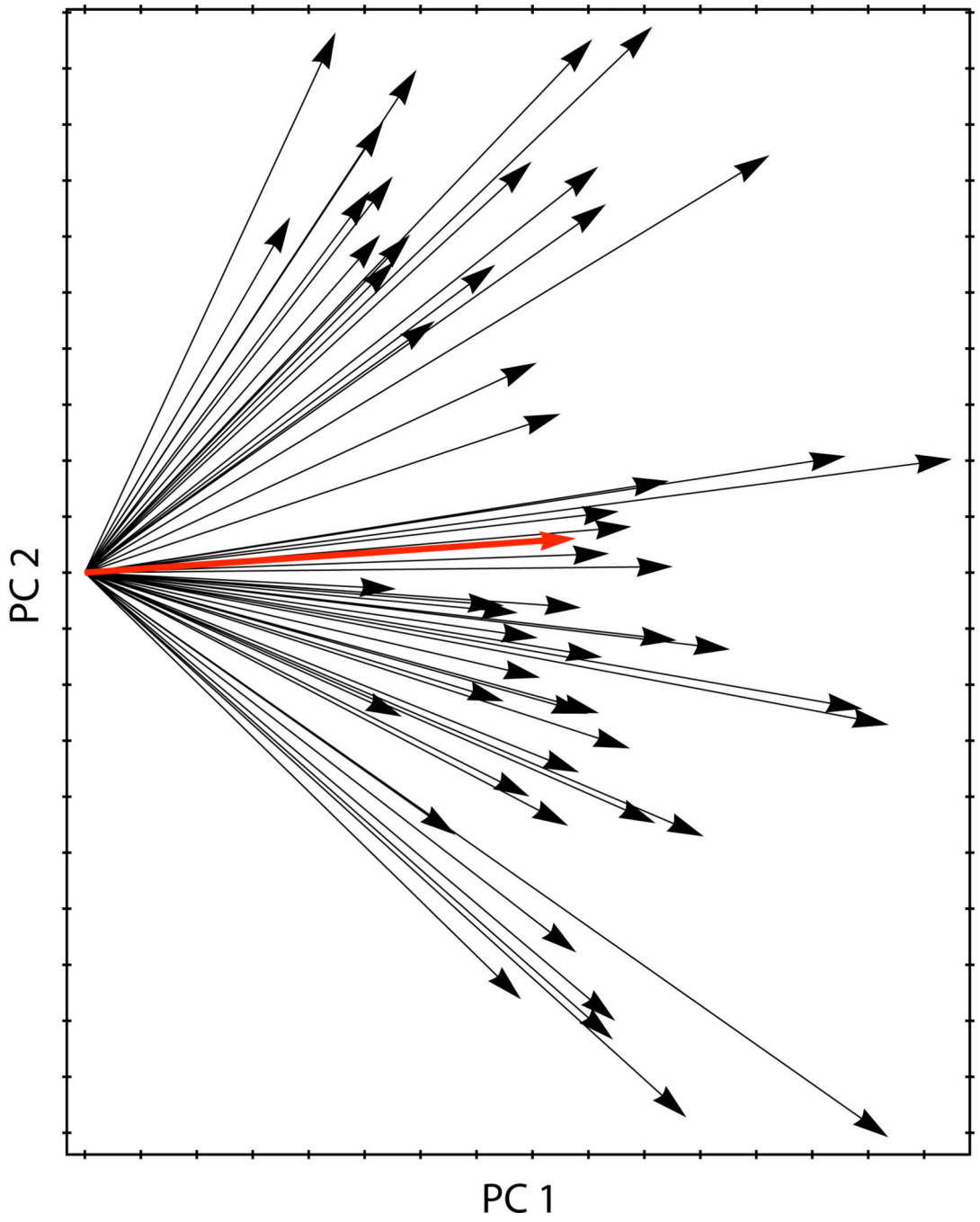

Figure 7.

First two principal components (PCs) of the non-additive deviation vectors (deviations of the offspring group mean shapes from the midpoint of the corresponding parental group means). In contrast to Figure 6, this PCA is not of all group means, but of the deviation vectors directly and computed to maximize variation around the origin (corresponding to zero deviation), not around the mean as in standard PCA. The average of these vectors (indicated by the red arrow) thus is closely aligned with PC1, along which all dominance vectors share a common direction. Further PCs do not significantly contribute to the pattern.

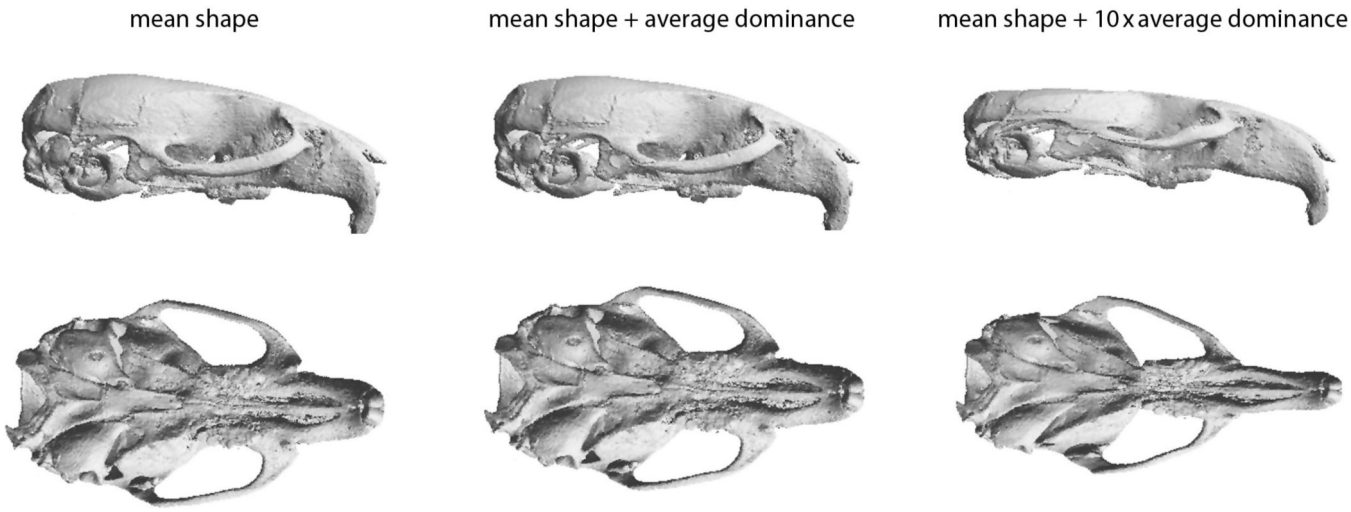

Figure 8.

Visualization of the average non-additive pattern (the shape deformation corresponding to the red arrow in Figure 7). Based on the measured landmarks, a surface model of a mouse skull is warped to the mean shape (left), the mean shape plus the average dominance vector (middle), and the mean shape plus 10 times the average dominance vector (right) to ease interpretation of the shape pattern. The color scheme facilitates recognition of the structure, and has no meaning in terms of deformation.

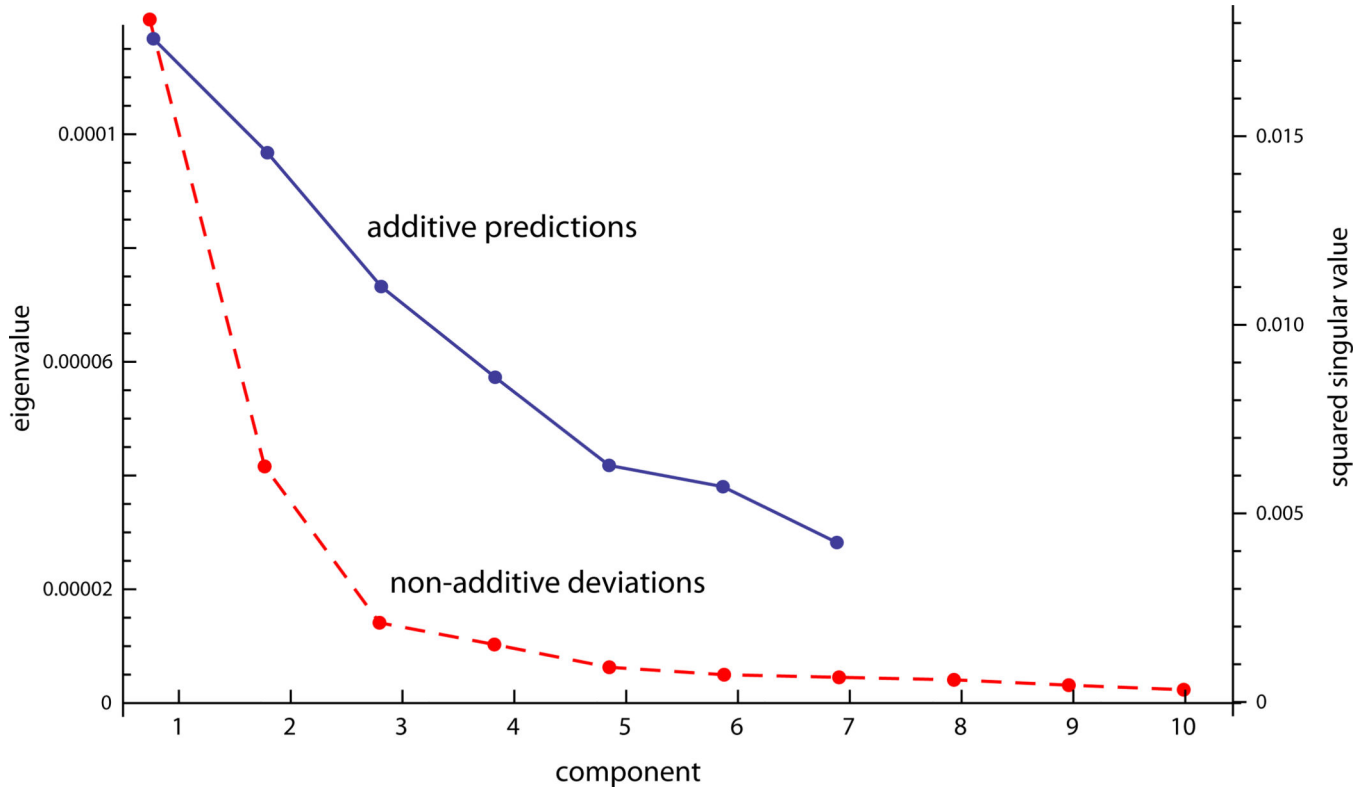

Figure 9.
Plot of the eigenvalues of the additive predictions and the non-additive deviations.

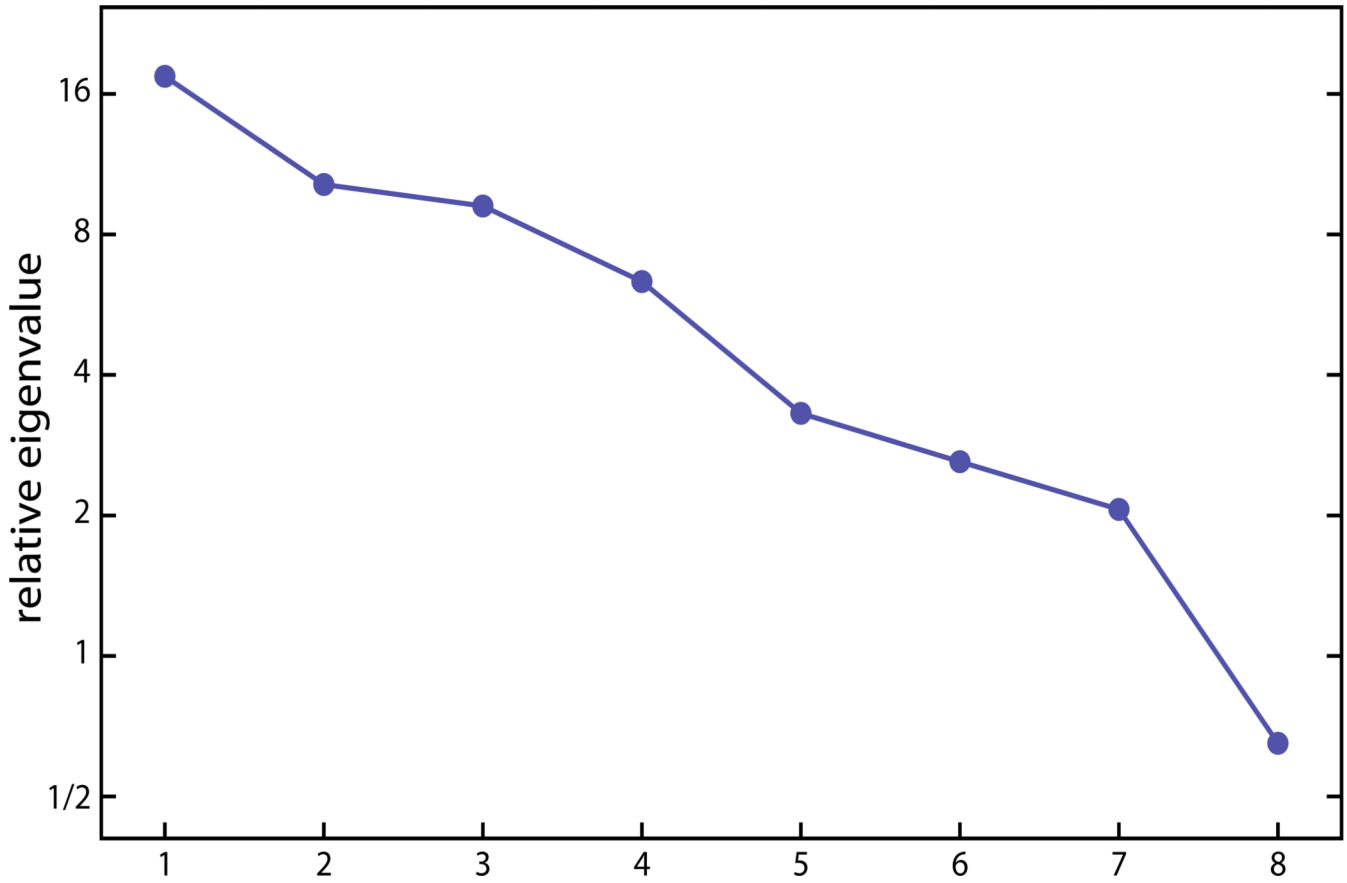

Figure 10.

Plot of the relative eigenvalues computed from the first eight principal components of the shape data. The relative eigenvalues correspond to ratios of genetic variance to environmental variance.

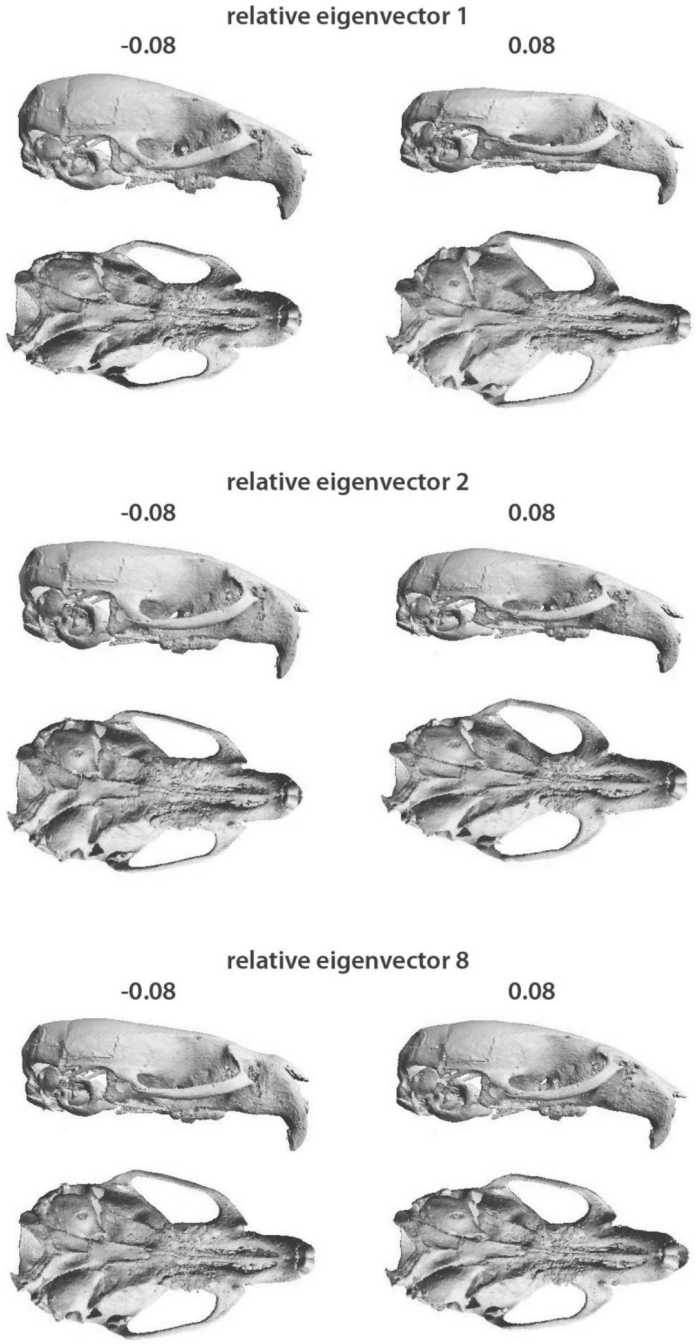

Figure 11.

Shape deformations visualizing the first, the second, and the last relative eigenvectors. These are the shape patterns with largest, second largest, and smallest genetic-to-environmental variance ratios, respectively. The color scheme facilitates recognition of the structure, and has no meaning in terms of deformation.

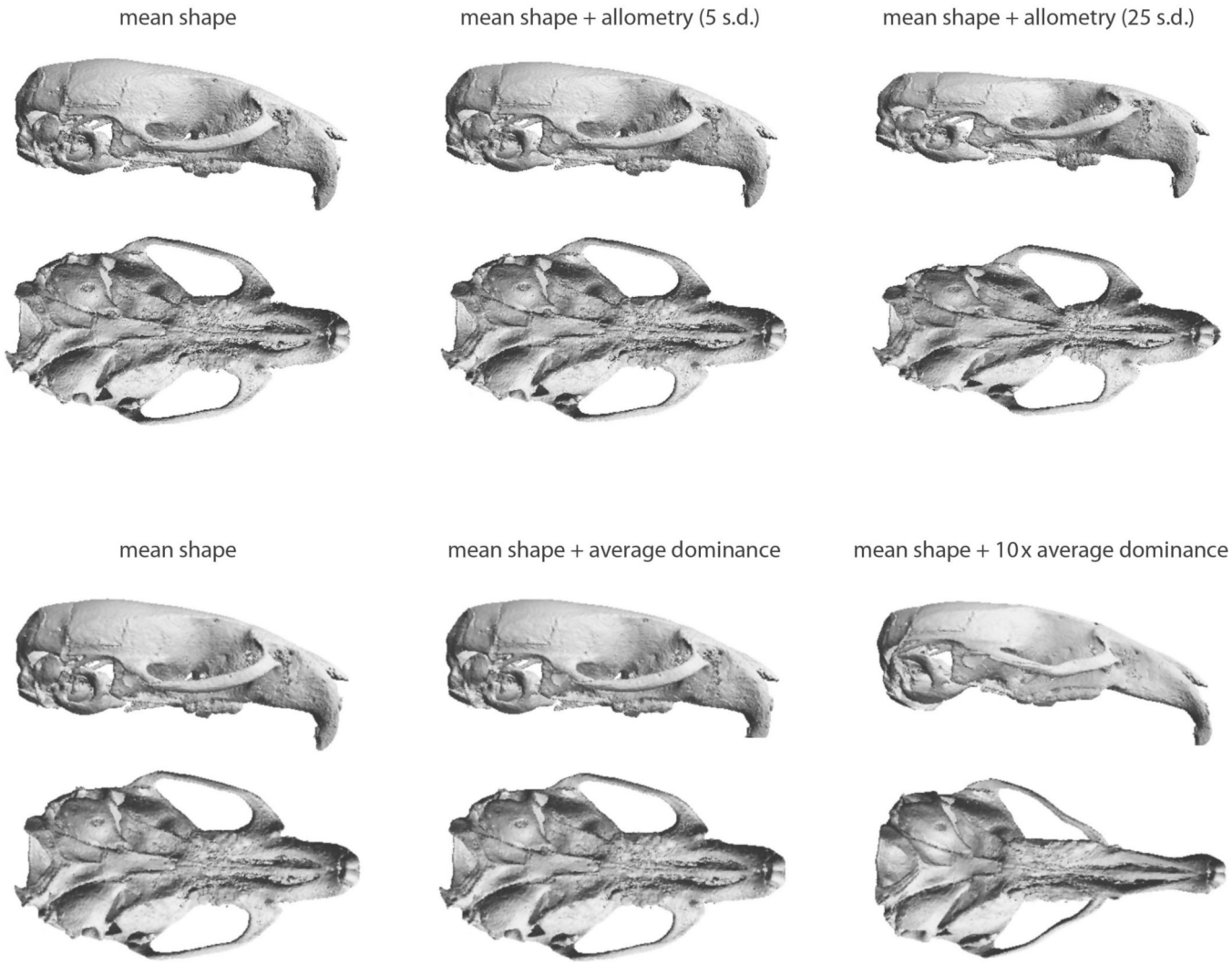

Figure 12.

(a) Visualization of the average within-group allometry. (b) Visualization of the average deviation from midparental shape computed from the residual data after allometry had been removed. The color scheme facilitates recognition of the structure, and has no meaning in terms of deformation.

Table 1

The list of inbred strains used as parentals in the diallel.

Code	Inbred parental strain	Short name	Relevant characteristics
AA		A/J	craniofacial and palate defects
BB		C57BL/6J	
CC		129S1/SvImJ	
DD		NOD/ShiLtJ	diabetes, non-obese
EE	New Zealand Obese	NZO/HILtJ	obese, mainly abdominal fat
FF	Castaneus	CAST/EiJ	low body weight
GG		PWK/PhJ	
HH		WSB/Ei	short face